Short Article

Structure

Regulation of Androgen Receptor Activity by Transient Interactions of Its Transactivation Domain with General Transcription Regulators

Graphical Abstract

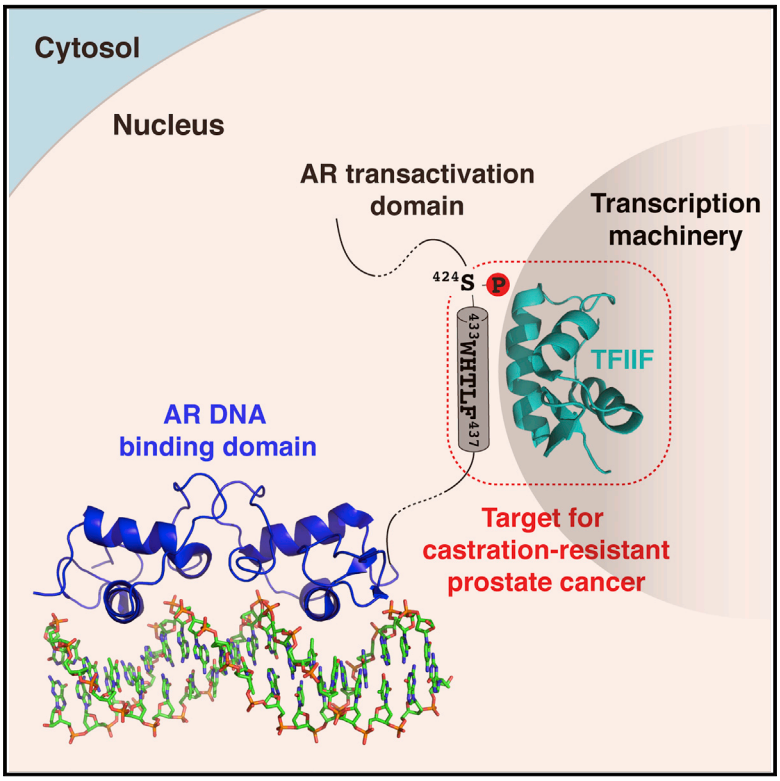

Highlights

- A short motif in transactivation unit 5 recruits the transcription machinery to the AR
- The motif is intrinsically disordered but folds into a helix upon binding
- Phosphorylation of Ser 424 of AR is essential for recruitment
- The interaction may be a target for castration-resistant prostate cancer

Authors

Eva De Mol, Elzbieta Szulc, Claudio Di Sanza, ..., Iain J. McEwan, Ángel R. Nebreda, Xavier Salvatella

Correspondence

xavier.salvatella@irbbarcelona.org

In Brief

Identifying ways to inhibit the androgen receptor (AR) is key for developing treatments for castration-resistant prostate cancer. Here, De Mol, Szulc et al. show that AR activity relies on transient interactions of a disordered motif with the transcription machinery and suggest therapeutic strategies for this disease.

De Mol et al., 2018, Structure *26*, 1–8
January 2, 2018
https://doi.org/10.1016/j.str.2017.11.007

CellPress

Please cite this article in press as: De Mol et al., Regulation of Androgen Receptor Activity by Transient Interactions of Its Transactivation Domain with General Transcription Regulators, Structure (2017), https://doi.org/10.1016/j.str.2017.11.007

Structure
Short Article

Regulation of Androgen Receptor Activity by Transient Interactions of Its Transactivation Domain with General Transcription Regulators

Eva De Mol,[1,8] Elzbieta Szulc,[1,8] Claudio Di Sanza,[1] Paula Martínez-Cristóbal,[1] Carlos W. Bertoncini,[1,6] R. Bryn Fenwick,[1,7] Marta Frigolé-Vivas,[1] Marianela Masín,[1,6] Irene Hunter,[2] Víctor Buzón,[1] Isabelle Brun-Heath,[1] Jesús García,[1] Gianni De Fabritiis,[3,4] Eva Estébanez-Perpiñá,[5] Iain J. McEwan,[2] Ángel R. Nebreda,[1,4] and Xavier Salvatella[1,4,9,*]

[1]Institute for Research in Biomedicine (IRB Barcelona), The Barcelona Institute of Science and Technology, Baldiri Reixac 10, 08028 Barcelona, Spain

[2]Institute of Medical Sciences, School of Medicine, Medical Sciences and Nutrition, University of Aberdeen, IMS Building, Foresterhill, Aberdeen AB25 2ZD, UK

[3]Computational Biophysics Laboratory (GRIB-IMIM), Universitat Pompeu Fabra, Barcelona Biomedical Research Park (PRBB), Doctor Aiguader 88, 08003 Barcelona, Spain

[4]ICREA, Passeig Lluís Companys 23, 08010 Barcelona, Spain

[5]Departament de Bioquímica i Biomedicina Molecular, Universitat de Barcelona and Institute of Biomedicine of the University of Barcelona (IBUB), Baldiri Reixac 15-21, 08028 Barcelona, Spain

[6]Present address: Instituto de Biología Molecular y Celular de Rosario (IBR), Consejo Nacional de Investigaciones Científicas y Técnicas (CONICET), Ocampo y Esmeralda, Rosario, Argentina

[7]Present address: Department of Integrative Structural and Computational Biology and the Skaggs Institute for Chemical Biology, The Scripps Research Institute, La Jolla, CA 92037, USA

[8]These authors contributed equally

[9]Lead Contact

*Correspondence: xavier.salvatella@irbbarcelona.org

https://doi.org/10.1016/j.str.2017.11.007

SUMMARY

The androgen receptor is a transcription factor that plays a key role in the development of prostate cancer, and its interactions with general transcription regulators are therefore of potential therapeutic interest. The mechanistic basis of these interactions is poorly understood due to the intrinsically disordered nature of the transactivation domain of the androgen receptor and the generally transient nature of the protein-protein interactions that trigger transcription. Here, we identify a motif of the transactivation domain that contributes to transcriptional activity by recruiting the C-terminal domain of subunit 1 of the general transcription regulator TFIIF. These findings provide molecular insights into the regulation of androgen receptor function and suggest strategies for treating castration-resistant prostate cancer.

INTRODUCTION

The activation of transcription relies on interactions between specific transcription factors and general transcription regulators that can be mediated by transcriptional co-activators (Fuda et al., 2009). It is important to characterize them because their inhibition by small molecules or other biological tools offers opportunities for therapeutic intervention in many disease areas, including oncology (Darnell, 2002). Since they involve intrinsically disordered (ID) transactivation domains, the associated complexes are however transient, marginally stable, and challenging to study (Wright and Dyson, 2015).

One case where inhibiting these interactions is appealing is castration-resistant prostate cancer (CRPC). This condition affects prostate cancer patients who are refractory to hormone therapy, which is based on preventing the activation of the androgen receptor (AR). The mechanisms that allow cell proliferation under these conditions are not yet fully characterized, but it is becoming clear that they include expression of constitutively active AR isoforms lacking the ligand binding domain (Robinson et al., 2015).

The complexes formed by the transactivation domain of AR (Lavery and McEwan, 2008a) and general transcription regulators are targets to interfere with CRPC (Sadar, 2011) because inhibiting their formation can lead to decreases in AR transcriptional activity and in the proliferation of prostate cancer cells. Here, we report the structural basis for the interaction of the transactivation domain of AR and the C-terminal domain of subunit 1 of the general transcription regulator TFIIF (RAP74-CTD), which involves the folding upon binding of a short motif in this receptor and contributes to transcriptional activity (Choudhry et al., 2006; McEwan and Gustafsson, 1997).

RESULTS

A Motif in Transcriptional Activation Unit 5 of AR Adopts a Helical Conformation to Recruit RAP74-CTD

To identify the regions of the AR involved in recruiting RAP74-CTD, we used solution nuclear magnetic resonance (NMR). NMR is appropriate for characterizing protein-protein interactions involving ID proteins because it provides residue-specific

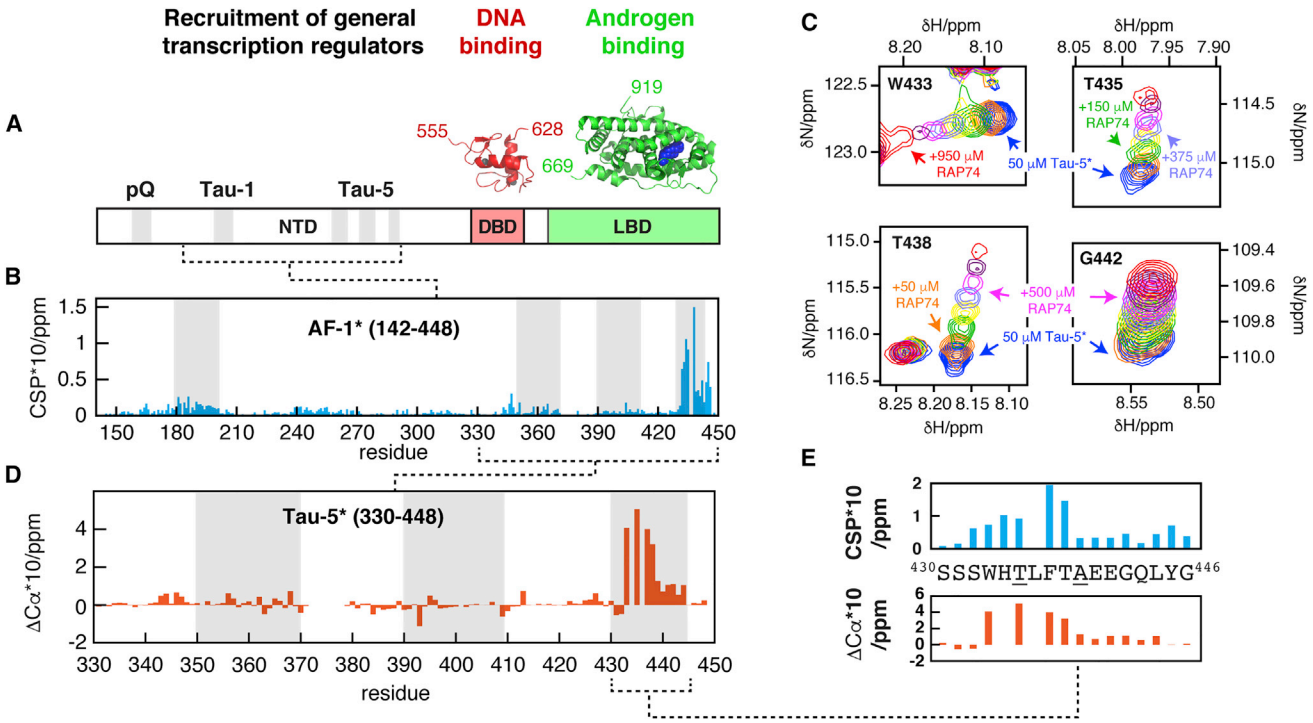

Figure 1. Identification of a Short Motif in AR that Recruits RAP74 by Adopting a Helical Structure

(A) Domain structure of AR indicating the regions that form the transactivation (NTD), DNA binding (DBD), and ligand binding (LBD) domains, as well as the polyGln tract (pQ) and the various partially folded motifs of the NTD (in gray) defined as those with a locally high transverse ^{15}N relaxation rate in NMR experiments (De Mol et al., 2016).

(B) Plot of the chemical shift perturbations (CSP) caused by 500 μM RAP74-CTD on the resonances of 50 μM AF-1* (residues 142–448) as a function of residue number ($CSP = \sqrt{\Delta\delta(H)^2 + (\Delta\delta(N)/5)^2}$) with an indication of the partially folded motifs (in gray).

(C) Changes in the resonances corresponding to four residues of Tau-5* (residues 330–448) at 50 μM titrated with 50 (orange), 150 (green), 250 (yellow), 375 (blue), 500 (pink), 710 (purple), and 950 (red) μM RAP74-CTD.

(D) Plot of the changes in ^{13}Cα chemical shift (ΔCα) caused by 500 μM RAP74-CTD* on the resonances of 100 μM Tau-5* with an indication of the partially folded motifs (in gray).

(E) Detail of the CSP and the ΔCα values obtained for specific residues in the interaction motif of AR with an indication, as underlined, of the positions used for hydrocarbon stapling (see below and Figure 3D).

See also Figure S1.

information in the absence of the long-range order required for crystallization (Dyson and Wright, 2004). In addition, it is well suited for the characterization of weak protein-protein interactions, which can occur when one of the partners is ID (Wright and Dyson, 2009).

We used a construct of the AR transactivation domain (AF1*, AR residues 142–448, Figure 1A) that contains two known functional subdomains, transcriptional activation units 1 and 5 (Tau-1 and -5) (Callewaert et al., 2006). AF1* is ID with regions of helical propensity in the structurally independent Tau-1 and Tau-5 subdomains (De Mol et al., 2016). We measured 2D ^{1}H,^{15}N heteronuclear single quantum coherence (HSQC) NMR spectra of AF-1* in the presence and in the absence of RAP74-CTD (RAP74 residues 450–517) (Lavery and McEwan, 2008a) and observed chemical shift perturbations in a region of Tau-5 with the sequence ^{431}SSWHTLFTAEEGQLYG^{446} (Figure 1B). To confirm that the interaction does not involve residues in Tau-1, we repeated the experiments with a shorter AR construct (Tau-5*, AR residues 330–448) and obtained an equivalent result (Figure S1A).

In order to estimate the stability of the complex, we performed a titration of Tau-5* with RAP74-CTD at 278 K (Figure 1C) and found that the affinity between these two proteins was in the millimolar range (Figure S1B). This is in agreement with the notion that the protein-protein interactions that activate transcription are weak due to their multivalent and transient nature (Melcher, 2000; Uesugi et al., 1997). To investigate whether binding of RAP74-CTD induces a conformational change in Tau-5, we compared the ^{13}Cα chemical shifts of Tau-5* in the presence and in the absence of its binding partner (RAP74-CTD*, see STAR Methods) by using 3D HNCA NMR experiments (Figure 1D). We observed increases in ^{13}Cα chemical shift in several residues of the motif, in agreement with the induction of a helical conformation (Neal et al., 2003), which were particularly large (ca. 0.5 ppm) for residues S432 to T438, which define two turns of an α helix (Figure 1E).

To identify the binding site of AR on the surface of RAP74-CTD, we performed ^{1}H,^{15}N HSQC experiments using RAP74-CTD (Nguyen et al., 2003a) and a peptide with sequence Ac-^{426}SA AASSSWHTLFTAEEGQLYG^{446}-NH_2. We observed chemical

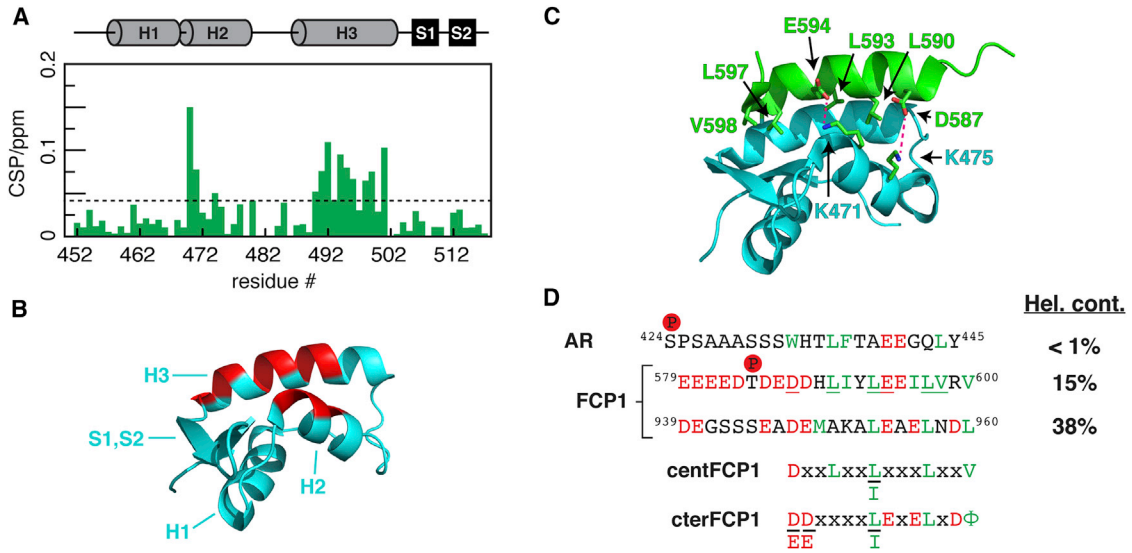

Figure 2. AR Binds to the Same Groove of RAP74-CTD as FCP1

(A) Plot of the chemical shift perturbations (CSP) caused by a peptide spanning the sequence of the AR motif (Ac-^{426}SAAASSSWHTLFTAEEGQLYG^{446}-NH_2) on the resonances of RAP74-CTD as a function of residue number with an indication, with a horizontal dashed line, of the threshold used for preparing (B).

(B) Solution structure of apo RAP74-CTD (Nguyen et al., 2003a) (PDB: 1NHA) indicating, in red, the residues whose resonances are most affected by binding of the AR motif (CSP >0.04 ppm).

(C) Structure of the complex formed by RAP74-CTD and the central motif of FCP1 (Yang et al., 2009) with an indication of the residues that are key for binding and of the main electrostatic interactions, shown in purple (PDB: 2K7L).

(D) Alignment of the sequences of the FCP1 and AR motifs interacting with RAP74-CTD indicating the acidic residues (in red), the hydrophobic residues (in green), the phosphosites identified so far (with the symbol P), the helical propensity predicted by Agadir (Muñoz and Serrano, 1994), and the consensus sequences centFCP1 and cterFCP1. The residues that are underlined in (D) correspond to those represented as sticks in (C).

See also Figure S2.

shift perturbations in helices H2 and H3 (Figures 2A and 2B), which define the binding groove of two ID motifs of FCP1 that fold into an α helix upon binding (Figure 2C) (Kamada et al., 2001, 2003; Nguyen et al., 2003a, 2003b; Yang et al., 2009). FCP1 is a nuclear phosphatase that dephosphorylates the C-terminal domain of RNA polymerase II and is recruited by RAP74-CTD at the termination of transcription (Archambault et al., 1997).

An analysis of the sequences of the disordered motifs of FCP1 (Figure 2D) and their conservation across species shows that the RAP74-CTD groove can accommodate motifs when these fulfill the requirements summarized in two consensus sequences (centFCP1 and cterFCP1) (Abbott et al., 2005; Yang et al., 2009). This emphasizes that the interaction with RAP74 relies on electrostatic interactions involving acidic residues at the N terminus and at the center of the motif and on hydrophobic interactions involving residues at relative positions *i/i+3/i+4*, which are buried in the interface (Figure 2C) (Kamada et al., 2001, 2003; Nguyen et al., 2003a, 2003b; Yang et al., 2009).

The AR motif partially fulfills the requirements summarized in centFCP1 and cterFCP1 (Figure 2D). It possesses hydrophobic residues in positions *i/i+3/i+4* (W433, L436, and F437) that can interact with the groove defined by helices H2 and H3 of RAP74-CTD and two acidic residues (E440 and E441) that can interact with the basic ones that surround the binding site (K471, K475, and K510, Figure 2C). To confirm their relevance for binding, we measured the chemical shift perturbations caused by two peptides, one with the three hydrophobic residues of the motif at positions *i/i+3/i+4* mutated to Ala (AHTAA, Ac-^{426}SAAASSSAHTAATAEEGQLYG^{446}-NH_2) and another with the two acidic residues mutated to Lys (KK, Ac-^{426}SAAASSSWHTLFTAKKGQLYG^{446}-NH_2). In both cases, we observed no chemical shift perturbations, confirming that these two features are key for binding (Figures S2A and S2B).

Helical Propensity and Phosphorylation State Determine the Stability of the Complex

The interaction between specific transcription factors and general transcription regulators can be enhanced by the binding of transcriptional co-activators (Fuxreiter et al., 2008) and by post-translational modifications (Gioeli and Paschal, 2012). The former can induce secondary structures in transactivation domains to facilitate their interaction with the basal transcription machinery (Lavery and McEwan, 2008a), and the latter can either stabilize the structural changes induced by binding (Bah et al., 2015) or directly stabilize the relevant complex (Bah and Forman-Kay, 2016). We used NMR to measure the affinity between RAP74-CTD and chemically modified peptides. This experimental setup allowed us to mimic the site-specific phosphorylations that occur during AR activation as well as by hydrocarbon stapling (Schafmeister et al., 2000) the helical secondary structure induced for example by co-activators.

The regions at the N terminus of the FCP1 motifs are rich in acidic side chains. However, the equivalent region in AR, which binds with lower affinity, is instead rich in Ser residues (^{424}SPSAAASSS^{432}, Figure 2D). We hypothesized that phosphorylations of this region contribute to stabilizing the transient

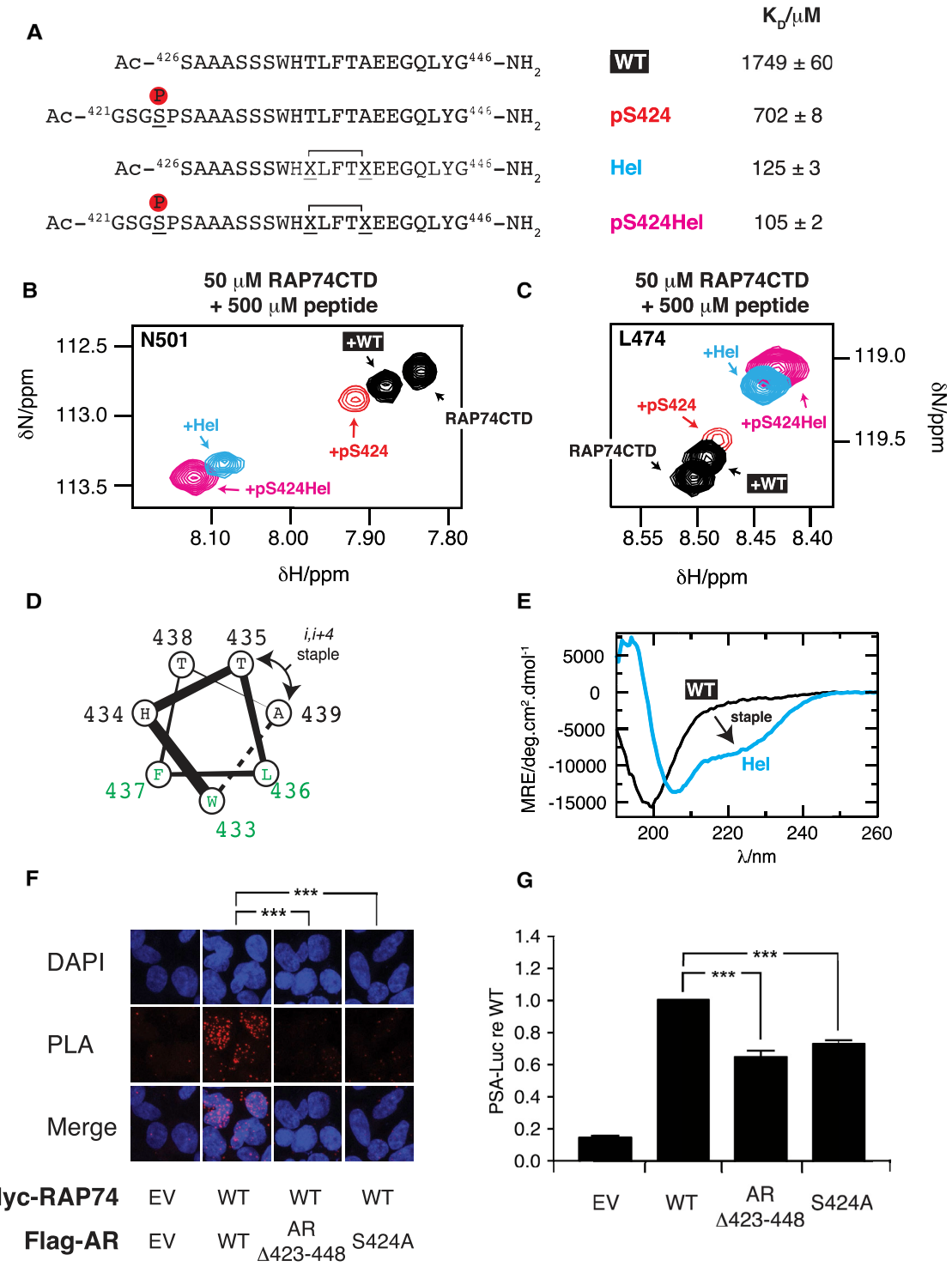

Figure 3. Determinants of the Interaction between AR and RAP74-CTD

(A) Sequences of peptides derived from the AR motif that recruits TFIIF, indicating affinities for RAP74-CTD (K_D). In Hel and pS424Hel, X represents the amino acid (*S*)-2-(4′-pentenyl)alanine and a continuous line links the residues stapled.

(B and C) Regions of the $^{1}H,^{15}N$ HSQC NMR spectrum of RAP-CTD illustrating the chemical shift perturbations caused by the peptides listed in (A) in residues N501 (B) and L474 (C) of RAP74-CTD.

(D) Helical wheel representation of the hydrophobic residues of the AR motif that recruits TFIIF with an illustration of the residues replaced by (*S*)-2-(4′-pentenyl) alanine and used for *i*,*i*+*4* stapling.

(E) CD spectrum of 50 μM solutions of the peptides WT and Hel.

(legend continued on next page)

complex that it forms with RAP74-CTD. An analysis of the known phosphosites of AR revealed that S424 is phosphorylated upon AR activation (Gioeli and Paschal, 2012). To determine whether this increases the stability of the transient complex, we measured the affinity for RAP74-CTD of a peptide phosphorylated on this position (pS424, Figure 3A–3C). The results indicated that phosphorylation of Ser 424 increased the affinity of the peptide from K_D = 1749 ± 60 μM to K_D = 702 ± 8 μM.

As shown in Figure 2D, an additional difference between the FCP1 and AR motifs is helical propensity. Whereas the central and C-terminal motifs of FCP1 have some helical propensity according to the predictor Agadir (Muñoz and Serrano, 1994) (15% and 38%), the AR motif has not (<1%), in agreement with our characterization of the structural properties of the NTD of AR (De Mol et al., 2016). Given that binding to the groove defined by helices H2 and H3 of RAP74-CTD involves the adoption of a helical conformation by the motif (Figures 1D, 1E, and 2C), we hypothesized that the low helical propensity of the AR motif contributes to its low affinity.

To determine the effect of increasing the helicity, we used hydrocarbon stapled peptides (Hel and pS424Hel, Figure 3A) where residues Thr 435 and Ala 439, which are in the face of the helix opposite the hydrophobic residues that interact with RAP74-CTD (Figure 3D), were replaced by (*S*)-2-(4′-pentenyl) alanine and stapled by olefin metathesis (Schafmeister et al., 2000). A comparison of the secondary structure of the wild-type (WT) and Hel peptides by circular dichroism (CD) (Figure 3E) confirmed that stapling indeed increased helical propensity. We analyzed the chemical shift perturbations caused in RAP74-CTD by Hel and pS424Hel, a stapled peptide including also the phosphorylation at S424, and confirmed that both interacted with higher affinity compared with their non-stapled counterparts (K_D = 125 ± 3 μM for Hel and K_D = 105 ± 2 μM, for pS424Hel, Figures 3A–3C). This confirms that phosphorylation facilitates binding of the AR motif and that processes that increase helical propensity can enhance AR transcriptional activity.

The Interaction Can Be Observed in Cells and Contributes to AR Transcriptional Activity

Although it is well established that TFIIF and the RAP74-CTD domain in particular interact with the AF1 domain of AR *in vitro* (Kumar et al., 2004; Lavery and McEwan, 2008b; McEwan and Gustafsson, 1997; Reid et al., 2002), there is little evidence that the interaction occurs in cells. To investigate this, we used biochemical techniques, such as co-immunoprecipitation, but failed to detect robust interaction presumably due to its transient nature. We next used the proximity ligation assay (PLA) (Söderberg et al., 2006), an immunofluorescence-based technique that allows the detection of proteins in close proximity inside cells.

For these studies, we tagged full-length AR and RAP74-CTD with Flag and Myc, respectively, transfected them in HEK293T cells, which do not express AR (see STAR Methods), and treated the cells with dihydrotestosterone (DHT) to cause the activation of the receptor. The results indicated that the two proteins interact (Figure 3F). To validate that the interaction takes place via the identified AR motif (AR 423–448), we carried out equivalent experiments with a mutant of AR with residues 423 to 448 removed (ARΔ423-448). In agreement with the results obtained *in vitro*, we observed a reduction of the interaction between ARΔ423-448 and RAP74-CTD in cells of ca. 40% (Figures 3F and S3D). We also investigated by PLA whether the phosphorylation of Ser 424 regulates the interaction with RAP74-CTD in cells by using an AR with Ser 424 mutated to Ala (S424A) and found that this was indeed the case (Figures 3F and S3D). Importantly, control immunofluorescence experiments showed that mutants ARΔ423–448 and S424A, like WT AR, are expressed and translocate to the nucleus upon activation by DHT (Figures S3A and S3B).

Finally, to further assess the functional relevance of the interaction between AR and RAP74-CTD via the motif identified in this work, we measured the transcriptional activity of WT AR and mutants ARΔ423–448 and S424A in HEK293T cells by means of a gene reporter assay (see STAR Methods). The results showed that deleting the motif or removing the phosphorylation site at position 424 lowered the transcriptional activity of AR by ca. 30% (Figures 3G and S3C).

DISCUSSION

The interactions between transactivation domains of specific transcription factors and transcriptional co-activators or general transcription regulators are among the best characterized examples of complexes involving ID proteins (Brzovic et al., 2011; Di Lello et al., 2006; Feng et al., 2009; Uesugi et al., 1997). Key features of these, which are present in the interaction studied here, are the induction of secondary structure upon interaction, their relatively weak nature, and the important role played by post-translational modifications in their regulation (Fuxreiter et al., 2008).

The interaction between AR and the C-terminal domain of subunit 1 of TFIIF is mediated by hydrophobic interactions between residues at positions *i/i+3/i+4* of the AR motif and a hydrophobic cleft on the surface of RAP74-CTD, with an important contribution of electrostatic interactions. This relative position of hydrophobic residues in the AR motif is common in transactivation domains, indicating that there could be a generic mechanism by which these domains recruit their binding partners and highlighting the general importance of regulatory mechanisms to provide specificity. We provide evidence that the phosphorylation of Ser 424 is important for the interaction between AR and RAP74-CTD and for transcriptional activity, illustrating how post-translational modifications can enhance the affinity and the specificity of ID proteins for their binding partners (Stein and Aloy, 2008).

Our results indicate that AR and FCP1 interact with the same groove in the structure of RAP74-CTD via similar motifs. The interaction between AR and RAP74-CTD is, as we have shown, important for transcriptional activity, whereas that between the latter and FCP1 is important for transcription termination (Archambault et al., 1997). The role of FCP1 in termination, which is carried out by its phosphatase domain, is to dephosphorylate the C-terminal

(F and G) The effect of deleting the AR motif (Δ423–448) and mutating Ser 424 to Ala (S424A) was assessed in HEK293T cells treated with 1 nM DHT by PLA to measure the interaction between AR and RAP74-CTD (F, see Figure S3D for a quantitative analysis) and by a reporter assay to measure AR transcriptional activity (G). In (F), EV stands for empty vector, and DAPI indicates the location of nuclei. In (G), the error bars represent the SE; ***$p < 0.001$.
See also Figure S3.

tail of RNA polymerase II, causing it to dissociate from the DNA and therefore allowing it to become involved in a subsequent round of transcription. We conclude that RAP74-CTD, which is a particularly dynamic part of the transcription machinery and is tethered to it via a very flexible linker (Sainsbury et al., 2015), uses a single binding mechanism to interact with different ID motifs at different stages of the process of transcription.

Our work indicates that the motif ^{431}SSWHTLFTAEEGQ LYG^{446} is important for the formation of the transient complex in cells but that its interaction with RAP74-CTD *in vitro* is weak, even after phosphorylation of Ser 424, unless a helical conformation is induced. Several mechanisms to induce a helical conformation in the motif can operate in cells, including an allosteric mechanism coupling the DNA-binding and transactivation domains upon DNA binding (Brodie and McEwan, 2005), a change in the conformation of the motif or the whole Tau-5 sub-domain after co-activator binding (Fuxreiter et al., 2008), or the effect of extrinsic factors that cannot be easily accounted for by *in vitro* studies. It is in fact possible that several of these mechanisms operate simultaneously as this would provide a means of regulating transcriptional activity (Hilser and Thompson, 2011; Wu and Fuxreiter, 2016).

The relevance of Tau-5, the sub-domain of the AR NTD where the ^{431}SSWHTLFTAEEGQLYG^{446} motif is found, for transcriptional activity in cells depends on the cell line used for the experiments and on the concentration of androgens to which the cells are exposed. Tau-5 inhibits transcriptional activity in prostate cancer cell lines expressing AR in the presence of physiological concentrations of androgens (Dehm et al., 2007). By contrast, it stimulates transcriptional activity in cell lines that do not express AR (Jenster et al., 1995) and, most importantly, in CRPC cell lines expressing AR in the absence of androgens or in their presence at castrate levels, where residues 433–437, at the core of the motif identified in this work, can act as an independent transactivation domain (Dehm et al., 2007). The reasons for this difference in behavior are currently not known and further work will be necessary to determine whether it is due, for example, to the action of specific co-regulators or to differences in post-translational modifications in AR.

Nevertheless, from a translational medicine point of view, our results and those available in the literature indicate that the motif that recruits RAP74-CTD can contribute to transcription activation by AR and, therefore, that the complex that it forms with this subunit of TFIIF is a potential therapeutic target for CRPC, although we cannot exclude the possibility that other interactions contribute to its function in transcription activation (Cato et al., 2017; He et al., 2000; Li et al., 2014). In summary, although protein-protein interactions involving ID proteins represent challenging targets for drug discovery, our work indicates that inhibitors of the recruitment of RAP74-CTD by AR, which could be either small molecules or peptides, could lead to treatments for CRPC (Yap et al., 2016).

STAR★METHODS

Detailed methods are provided in the online version of this paper and include the following:

- KEY RESOURCES TABLE
- CONTACT FOR REAGENT AND RESOURCE SHARING
- EXPERIMENTAL MODEL AND SUBJECT DETAILS
- METHOD DETAILS
  - Protein Expression and Purification
  - Handling of Peptides
  - NMR
  - Fitting of the NMR Data to Obtain the Values of K_D
  - Cell Culture and Transfection
  - Plasmids
  - Western Blot Analyses
  - Proximity Ligation Assay (PLA)
  - Localization Studies
  - Transcriptional Activity Assay
- QUANTIFICATION AND STATISTICAL ANALYSIS

SUPPLEMENTAL INFORMATION

Supplemental Information includes three figures and can be found with this article online at https://doi.org/10.1016/j.str.2017.11.007.

AUTHOR CONTRIBUTIONS

E.D.M., E.S., C.D.S., P.M.-C., and C.W.B. designed, carried out, analyzed and interpreted the experiments, and contributed to writing the manuscript. R.B.F., M.F.-V., M.M., I.H., V.B., J.G., G.D.F., and E.E.-P. provided experimental support. I.B.-H., I.J.M., and A.R.N. contributed to analyzing and interpreting the experiments as well as to writing the manuscript. X.S. designed and contributed to interpreting the experiments as well as to writing the manuscript.

ACKNOWLEDGMENTS

The authors thank Miquel Pons, Philipp Selenko, and Peter Wright for helpful discussions as well as Joan Miquel Valverde (IRB) and the ICTS NMR facility, managed by the scientific and technological centers of the University of Barcelona (CCiT UB), for their help in protein production and NMR. They also thank the IRB protein expression core facility for its assistance in cloning, the IRB advanced microscopy facility for assistance in immunofluorescence and PLA, and the IRB biostatistics and bioinformatics facility for assistance in the analysis of the gene reporter and PLA data. This work was supported by IRB, ICREA (X.S.), Obra Social "la Caixa" (E.D.M., E.S., and X.S.), MINECO (BIO2012-31043 and BIO2015-70092-R to X.S., BIO2014-53095-P to G.D.F.), Marató de TV3 (102030 to X.S. and 102031 to E.E.-P), the COFUND program of the European Commission (C.D.S.), the European Research Council (CONCERT, contract number 648201 to X.S.), the Ramón y Cajal program of MICINN (RYC-2011-07873 to C.W.B.), the Serra Hunter Program (E.E.-P.), AGAUR (SGR-2014-56RR14 to E.E.-P), and FEDER (G.D.F.). I.H. was supported by funding from the Chief Scientist's Office of the Scottish Government (ETM-258, ETM-382). IRB Barcelona is the recipient of a Severo Ochoa Award of Excellence from MINECO (Government of Spain).

Received: August 1, 2017
Revised: October 12, 2017
Accepted: November 10, 2017
Published: December 7, 2017

REFERENCES

Abbott, K.L., Renfrow, M.B., Chalmers, M.J., Nguyen, B.D., Marshall, A.G., Legault, P., and Omichinski, J.G. (2005). Enhanced binding of RNAP II CTD phosphatase FCP1 to RAP74 following CK2 phosphorylation. Biochemistry *44*, 2732–2745.

Archambault, J., Chambers, R.S., Kobor, M.S., Ho, Y., Cartier, M., Bolotin, D., Andrews, B., Kane, C.M., and Greenblatt, J. (1997). An essential component of a C-terminal domain phosphatase that interacts with transcription factor IIF in Saccharomyces cerevisiae. Proc. Natl. Acad. Sci. USA *94*, 14300–14305.

Bah, A., and Forman-Kay, J.D. (2016). Modulation of intrinsically disordered protein function by post-translational modifications. J. Biol. Chem. *291*, 6696–6705.

Bah, A., Vernon, R.M., Siddiqui, Z., Krzeminski, M., Muhandiram, R., Zhao, C., Sonenberg, N., Kay, L.E., and Forman-Kay, J.D. (2015). Folding of an intrinsically disordered protein by phosphorylation as a regulatory switch. Nature *519*, 106–109.

Brodie, J., and McEwan, I.J. (2005). Intra-domain communication between the N-terminal and DNA-binding domains of the androgen receptor: modulation of androgen response element DNA binding. J. Mol. Endocrinol. *34*, 603–615.

Brzovic, P.S., Heikaus, C.C., Kisselev, L., Vernon, R., Herbig, E., Pacheco, D., Warfield, L., Littlefield, P., Baker, D., Klevit, R.E., et al. (2011). The acidic transcription activator Gcn4 binds the mediator subunit Gal11/Med15 using a simple protein interface forming a fuzzy complex. Mol. Cell *44*, 942–953.

Callewaert, L., Van Tilborgh, N., and Claessens, F. (2006). Interplay between two hormone-independent activation domains in the androgen receptor. Cancer Res. *66*, 543–553.

Cato, L., Neeb, A., Sharp, A., Buzón, V., Ficarro, S.B., Yang, L., Muhle-Goll, C., Kuznik, N.C., Riisnaes, R., Nava Rodrigues, D., et al. (2017). Development of Bag-1L as a therapeutic target in androgen receptor-dependent prostate cancer. Elife *6*, e27159.

Choudhry, M.A., Ball, A., and McEwan, I.J. (2006). The role of the general transcription factor IIF in androgen receptor-dependent transcription. Mol. Endocrinol. *20*, 2052–2061.

Darnell, J.E., Jr. (2002). Transcription factors as targets for cancer therapy. Nat. Rev. Cancer *2*, 740–749.

Dehm, S.M., Regan, K.M., Schmidt, L.J., and Tindall, D.J. (2007). Selective role of an NH2-terminal WxxLF motif for aberrant androgen receptor activation in androgen depletion independent prostate cancer cells. Cancer Res. *67*, 10067–10077.

De Mol, E., Fenwick, R.B., Phang, C.T.W., Buzón, V., Szulc, E., de la Fuente, A., Escobedo, A., García, J., Bertoncini, C.W., Estébanez-Perpiñá, E., et al. (2016). EPI-001, a compound active against castration-resistant prostate cancer, targets transactivation unit 5 of the androgen receptor. ACS Chem. Biol. *11*, 2499–2505.

Di Lello, P., Jenkins, L.M.M., Jones, T.N., Nguyen, B.D., Hara, T., Yamaguchi, H., Dikeakos, J.D., Appella, E., Legault, P., and Omichinski, J.G. (2006). Structure of the Tfb1/p53 complex: insights into the interaction between the p62/Tfb1 subunit of TFIIH and the activation domain of p53. Mol. Cell *22*, 731–740.

Dyson, H.J., and Wright, P.E. (2004). Unfolded proteins and protein folding studied by NMR. Chem. Rev. *104*, 3607–3622.

Feng, H., Jenkins, L.M.M., Durell, S.R., Hayashi, R., Mazur, S.J., Cherry, S., Tropea, J.E., Miller, M., Wlodawer, A., Appella, E., et al. (2009). Structural basis for p300 Taz2-p53 TAD1 binding and modulation by phosphorylation. Structure *17*, 202–210.

Fuda, N.J., Ardehali, M.B., and Lis, J.T. (2009). Defining mechanisms that regulate RNA polymerase II transcription in vivo. Nature *461*, 186–192.

Fuxreiter, M., Tompa, P., Simon, I., Uversky, V.N., Hansen, J.C., and Asturias, F.J. (2008). Malleable machines take shape in eukaryotic transcriptional regulation. Nat. Chem. Biol. *4*, 728–737.

Gioeli, D., and Paschal, B.M. (2012). Post-translational modification of the androgen receptor. Mol. Cell. Endocrinol *352*, 70–78.

He, B., Kemppainen, J.A., and Wilson, E.M. (2000). FXXLF and WXXLF sequences mediate the NH2-terminal interaction with the ligand binding domain of the androgen receptor. J. Biol. Chem. *275*, 22986–22994.

Hilser, V.J., and Thompson, E.B. (2011). Structural dynamics, intrinsic disorder, and allostery in nuclear receptors as transcription factors. J. Biol. Chem. *286*, 39675–39682.

Jenster, G., van der Korput, H.A., Trapman, J., and Brinkmann, A.O. (1995). Identification of two transcription activation units in the N-terminal domain of the human androgen receptor. J. Biol. Chem. *270*, 7341–7346.

Kamada, K., De Angelis, J., Roeder, R.G., and Burley, S.K. (2001). Crystal structure of the C-terminal domain of the RAP74 subunit of human transcription factor IIF. Proc. Natl. Acad. Sci. USA *98*, 3115–3120.

Kamada, K., Roeder, R.G., and Burley, S.K. (2003). Molecular mechanism of recruitment of TFIIF- associating RNA polymerase C-terminal domain phosphatase (FCP1) by transcription factor IIF. Proc. Natl. Acad. Sci. USA *100*, 2296–2299.

Kumar, R., Betney, R., Li, J., Thompson, E.B., and McEwan, I.J. (2004). Induced alpha-helix structure in AF1 of the androgen receptor upon binding transcription factor TFIIF. Biochemistry *43*, 3008–3013.

Lavery, D.N., and McEwan, I.J. (2008a). Structural characterization of the native NH2-terminal transactivation domain of the human androgen receptor: a collapsed disordered conformation underlies structural plasticity and protein-induced folding. Biochemistry *47*, 3360–3369.

Lavery, D.N., and McEwan, I.J. (2008b). Functional characterization of the native NH2-terminal transactivation domain of the human androgen receptor: binding kinetics for interactions with TFIIF and SRC-1a. Biochemistry *47*, 3352–3359.

Li, N., Chen, M., Truong, S., Yan, C., and Buttyan, R. (2014). Determinants of Gli2 co-activation of wildtype and naturally truncated androgen receptors. Prostate *74*, 1400–1410.

McEwan, I.J., and Gustafsson, J. (1997). Interaction of the human androgen receptor transactivation function with the general transcription factor TFIIF. Proc. Natl. Acad. Sci. USA *94*, 8485–8490.

Melcher, K. (2000). The strength of acidic activation domains correlates with their affinity for both transcriptional and non-transcriptional proteins. J. Mol. Biol. *301*, 1097–1112.

Muñoz, V., and Serrano, L. (1994). Elucidating the folding problem of helical peptides using empirical parameters. Nat. Struct. Biol. *1*, 399–409.

Neal, S., Nip, A.M., Zhang, H., and Wishart, D.S. (2003). Rapid and accurate calculation of protein 1H, 13C and 15N chemical shifts. J. Biomol. NMR *26*, 215–240.

Nguyen, B.D., Chen, H.-T., Kobor, M.S., Greenblatt, J., Legault, P., and Omichinski, J.G. (2003a). Solution structure of the carboxyl-terminal domain of RAP74 and NMR characterization of the FCP1-binding sites of RAP74 and human TFIIB. Biochemistry *42*, 1460–1469.

Nguyen, B.D., Abbott, K.L., Potempa, K., Kobor, M.S., Archambault, J., Greenblatt, J., Legault, P., and Omichinski, J.G. (2003b). NMR structure of a complex containing the TFIIF subunit RAP74 and the RNA polymerase II carboxyl-terminal domain phosphatase FCP1. Proc. Natl. Acad. Sci. USA *100*, 5688–5693.

Reid, J., Murray, I., Watt, K., Betney, R., and McEwan, I.J. (2002). The androgen receptor interacts with multiple regions of the large subunit of general transcription factor TFIIF. J. Biol. Chem. *277*, 41247–41253.

Robinson, D., Van Allen, E.M., Wu, Y.-M., Schultz, N., Lonigro, R.J., Mosquera, J.-M., Montgomery, B., Taplin, M.-E., Pritchard, C.C., Attard, G., et al. (2015). Integrative clinical genomics of advanced prostate cancer. Cell *161*, 1215–1228.

Sadar, M.D. (2011). Small molecule inhibitors targeting the "Achilles' heel" of androgen receptor activity. Cancer Res. *71*, 1208–1213.

Sainsbury, S., Bernecky, C., and Cramer, P. (2015). Structural basis of transcription initiation by RNA polymerase II. Nat. Rev. Mol. Cell Biol. *16*, 129–143.

Schafmeister, C.E., Po, J., and Verdine, G.L. (2000). An all-hydrocarbon cross-linking system for enhancing the helicity and metabolic stability of peptides. J. Am. Chem. Soc. *122*, 5891–5892.

Söderberg, O., Gullberg, M., Jarvius, M., Ridderstråle, K., Leuchowius, K.-J., Jarvius, J., Wester, K., Hydbring, P., Bahram, F., Larsson, L.-G., et al. (2006). Direct observation of individual endogenous protein complexes in situ by proximity ligation. Nat. Methods *3*, 995–1000.

Stein, A., and Aloy, P. (2008). Contextual specificity in peptide-mediated protein interactions. PLoS One *3*, e2524.

Stenoien, D.L., Cummings, C.J., Adams, H.P., Mancini, M.G., Patel, K., DeMartino, G.N., Marcelli, M., Weigel, N.L., and Mancini, M.A. (1999).

Polyglutamine-expanded androgen receptors form aggregates that sequester heat shock proteins, proteasome components and SRC-1, and are suppressed by the HDJ-2 chaperone. Hum. Mol. Genet. *8*, 731–741.

Uesugi, M., Nyanguile, O., Lu, H., Levine, A.J., and Verdine, G.L. (1997). Induced alpha helix in the VP16 activation domain upon binding to a human TAF. Science *277*, 1310–1313.

Vandepoele, K., Van Roy, N., Staes, K., Speleman, F., and van Roy, F. (2005). A novel gene family NBPF: intricate structure generated by gene duplications during primate evolution. Mol. Biol. Evol. *22*, 2265–2274.

Wright, P.E., and Dyson, H.J. (2009). Linking folding and binding. Curr. Opin. Struct. Biol. *19*, 31–38.

Wright, P.E., and Dyson, H.J. (2015). Intrinsically disordered proteins in cellular signalling and regulation. Nat. Rev. Mol. Cell Biol. *16*, 18–29.

Wu, H., and Fuxreiter, M. (2016). The structure and dynamics of higher-order assemblies: amyloids, signalosomes, and granules. Cell *165*, 1055–1066.

Yang, A., Abbott, K.L., Desjardins, A., Di Lello, P., Omichinski, J.G., and Legault, P. (2009). NMR structure of a complex formed by the carboxyl-terminal domain of human RAP74 and a phosphorylated peptide from the central domain of the FCP1 phosphatase. Biochemistry *48*, 1964–1974.

Yap, T.A., Smith, A.D., Ferraldeschi, R., Al-Lazikani, B., Workman, P., and de Bono, J.S. (2016). Drug discovery in advanced prostate cancer: translating biology into therapy. Nat. Rev. Drug Discov. *15*, 699–718.

STAR★METHODS

KEY RESOURCES TABLE

REAGENT or RESOURCE	SOURCE	IDENTIFIER
Antibodies		
Anti-β-actin-HRP	Abcam	Ab8224; RRID: AB_449644
Anti-AR (N-20)	Santa Cruz	sc-816; RRID: AB_1563391
Rabbit-anti-Flag	Sigma	F7425; RRID: AB_439687
Mouse-anti-Myc	Abcam	ab32; RRID: AB_303599
Goat anti-rabbit Alexa-Fluor 568	Invitrogen	A11036; RRID: AB_10563566
Bacterial and Virus Strains		
Rosetta™(DE3)pLysS Competent Cells	Novagen	Cat# 70956
Chemicals, Peptides, and Recombinant Proteins		
Recombinant protein: human AR AF-1* (aa 142-448, ref# P10275)	(De Mol et al., 2016)	N/A
Recombinant protein: human AR Tau-5* (aa 330-448, ref# P10275)	(De Mol et al., 2016)	N/A
Recombinant protein: human RAP74-CTD (aa 450-517, ref# NP35269)	This paper	N/A
Recombinant protein: human RAP74-CTD* (aa 363-517, ref# NP35269)	(Lavery and McEwan, 2008b)	N/A
Synthetic WT peptide: Ac-SAAASSSWHTLFTAEEGQLYG-NH2	Synthesized by ICTS NANBIOSIS	N/A
Synthetic AHTAA peptide: Ac-SAAASSSAHTAATAEE GQLYG-NH2	Synthesized by ICTS NANBIOSIS	N/A
Synthetic KK peptide: Ac-SAAASSSWHTLFTAKKGQLYG-NH2	Synthesized by ICTS NANBIOSIS	N/A
Synthetic pS424 peptide: Ac-GSGpSPSAAASSSWHTLFTA EEGQLYG-NH2	Synthesized by Genscript	N/A
Synthetic Hel peptide: Ac-SAAASSSWHXLFTXEEGQ LYG446-NH2	Synthesized by Genscript and ICTS NANBIOSIS	N/A
Synthetic pS424Hel peptide: Ac-GSGpSPSAAASSSWHXLFTXE EGQLYG-NH2	Synthesized by ICTS NANBIOSIS	N/A
Dulbecco's Modified Eagle Medium (DMEM)	Gibco	Cat# 41966-052
Fetal Bovin Serum (FBS)	Gibco	Cat#10270-106
Charcoal Stripped FBS (CSS)	Gibco	Cat# 12676011
Critical Commercial Assays		
Duolink In Situ PLA Probe Anti-Rabbit PLUS	Sigma	Cat# DUO92002
Duolink In Situ PLA Probe Anti-Mouse MINUS	Sigma	Cat# DUO92004
Duolink In Situ Detection Reagents Orange	Sigma	Cat# DUO92007
Dual-Luciferase Reporter Assay System	Promega	Cat# E1910
Deposited Data		
NMR assignments of RAP74-CTD	BMRB (www.bmrb.wisc.edu)	27288
Experimental Models: Cell Lines		
Human Embryonic Kidney 293T cells	ATCC	CRL-3216
Recombinant DNA		
pDONR221-RAP74CTD	GeneArt	N/A
pDEST-HisBMP	(Nallamsetty et al., 2005)	Addgene 11085
pDEST-Myc	(Vandepoele et al. 2005)	LMBP 4541
pDEST-Myc-RAP74CTD	This paper	N/A
pEFGFP-C1-AR	(Stenoien et al., 1999)	Addgene 28235
pCMV5-FLAG	Sigma-Aldrich	Cat# E6908
Flag-AR	This paper	N/A
ARΔ423-448	This paper	N/A

(*Continued on next page*)

Continued

REAGENT or RESOURCE	SOURCE	IDENTIFIER
S424A	This paper	N/A
PSA(6.1)–Luc	Hsieh lab	N/A
pTK-Renilla	Promega	Cat# E224A
Oligonucleotides		
Primers for S424A mutant generation Fw: 5'-GGACCCGGTTCTGGGGCACCCTCAGCCGCCGC-3' Rv: 5'-GCGGCGGCTGAGGGTGCCCCAGAACCGGGTCC-3'	This paper	N/A
Primers for ARΔ423-448 mutant generation Fw: 5'-CGGGACCCGGTTCTGGGTCAGGTGGTGGGGGTG GTGGCGG-3' Rv: 5'-CCGCCACCACCCCCACCACC↓TGACCCAGAACC GGGTCCCG-3'	This paper	N/A
Software and Algorithms		
GraphPad Prism	GraphPad Software (www.graphpad.com)	7.0

CONTACT FOR REAGENT AND RESOURCE SHARING

Further information and requests for resources and reagents should be directed to and will be fulfilled by the Lead Contact, Xavier Salvatella (xavier.salvatella@irbbarcelona.org).

EXPERIMENTAL MODEL AND SUBJECT DETAILS

Rosetta™(DE3)pLysS Competent Cells were used for protein expression. Human Embryonic Kidney 293T cells (HEK293T cells) were maintained in DMEM containing 4.5 g/L D-glucose, pyruvate and L-glutamine (Life Technologies) supplemented with 10% Charcoal-stripped FBS (Life Technologies), 100 g·ml-1 of penicillin and 100g·ml-1 of streptomycin. Cells were cultured in a humidified atmosphere containing 5% CO2 at 37°C.

METHOD DETAILS

Protein Expression and Purification

For the preparation of samples of RAP74-CTD for NMR experiments a synthetic gene corresponding to residues 450 to 517 of RAP74 and including a cleavage site for TEV protease, at the N-terminus, was purchased from GeneArt cloned to a pDONR221vector and sub-cloned into a pDEST-HisMBP vector for protein expression, obtained from Addgene (Nallamsetty et al., 2005). Cells Rosetta cells were grown at 37°C in LB medium for the production of non-isotopically labeled samples. For single (^{15}N) or double (^{15}N,^{13}C) isotopic labeling, cells were grown in minimal MOPS medium containing $^{15}NH_4Cl$ or $^{15}NH_4Cl$ and ^{13}C-glucose, respectively as nitrogen and carbon sources. Protein expression was induced with 1 mM IPTG at OD_{600nm} 0.7. After 3 hours cells were harvested by centrifugation and resuspended in lysis buffer (50 mM Tris-HCl pH 8.0, 1 M NaCl, 10 mM imidazole). The soluble fraction was loaded onto a Ni^{2+} affinity chromatography column (GE) and eluted in lysis buffer with an imidazole gradient. The eluted RAP74-CTD was pooled, concentrated and dialyzed for 16 hours against 50 mM Tris-HCl pH 8.0, 200 mM NaCl. After dialysis, EDTA was added to a final concentration of 0.5 mM and the protein was incubated with TEV protease for 16 hours at 4 °C. The HisMBP moiety and the uncleaved material were removed by reverse Ni^{2+} chromatography, which was followed by cationic exchange and size exclusion chromatography steps. AF-1*, Tau-5* and RAP74-CTD* were produced following procedures reported previously (De Mol et al., 2016; Lavery and McEwan, 2008b).

Handling of Peptides

The lyophilized peptides were dissolved in deionized water or directly in 20 mM sodium phosphate, 0.01% (w/v) NaN_3 and the pH of the resulting solution was adjusted by addition of concentrated NaOH. The concentration of these solutions was determined by amino acid analysis. The CD spectra of 50 μM solutions of peptides WT and Hel in 20 mM sodium phosphate pH 7.4, were measured in a JASCO spectropolarimeter at 293 K by using a 1 mm path length quartz cuvette.

NMR

NMR spectra were recorded on 600 and 800 MHz Bruker Avance spectrometers equipped with cryoprobes. Backbone assignments for RAP74-CTD were obtained using three-dimensional HNCO, HN(CA)CO, HNCA, HN(CO)CA, CBCANH and CBCA(CO)NH spectra acquired on a 0.5 mM ^{15}N,^{13}C-double labeled sample and have been deposited in the BMRB with accession code 27288. Chemical

shifts were referenced by using 3-(trimethylsilyl)-1-propanesulfonic acid sodium salt (DSS) as internal reference. $^{1}H,^{15}N$-HSQC and HNCA spectra of the AF-1* and Tau-5* in the presence of increasing amounts of unlabeled RAP74-CTD were obtained at 278 K in 20 mM sodium phosphate (pH 7.4), 1 mM TCEP, 10% D_2O, and 30 μM DSS. To study the interaction of RAP74-CTD with peptides, $^{1}H,^{15}N$-HSQC spectra were acquired at 298 K with samples containing uniformly ^{15}N-labeled RAP74-CTD (50 μM) and the indicated amount of peptide dissolved in 20 mM sodium phosphate, 0.01% (w/v) NaN_3, 30 μM DSS, 10% D_2O at pH 7.4.

Fitting of the NMR Data to Obtain the Values of K_D

The changes in ^{1}H and ^{15}N chemical shift ($\Delta\delta_i$) caused by synthetic peptides in RAP74-CTD were globally fit to the following isotherm by using GraphPad Prism to obtain the value of K_D, where C is the concentration of titrand, n is the ratio between the concentration of titrant and that of titrand and $\Delta\delta_i^{sat}$ is the difference in chemical shift, for nucleus i, between the free and bound titrand.

$$\Delta\delta_i = \frac{\Delta\delta_i^{sat}}{2}\left(1 + K_D/C + n - \sqrt{(1+n+K_D/C)^2 - 4n}\right)$$

Cell Culture and Transfection

Transient transfection of HEK293T cells was performed with polyethylenimine (PEI, Polysciences) at a ratio of 1 μg DNA to 3 μl PEI.

Plasmids

The sequence coding for AR from the plasmid pEGFP-C1-AR (Stenoien et al., 1999), was subcloned into *Bgl* II/ *Sal* I sites of a pCMV5-FLAG vector to give Flag-AR. The ARΔ423-448 and S424A mutants were generated by site-directed mutagenesis. The sequence coding for RAP74 CTD from the plasmid pDONR221-RAP74 CTD was sub-cloned into a pDEST-Myc vector to give pDEST-Myc-Rap74 CTD.

Western Blot Analyses

Flag-AR wild type as well as AR mutants ARΔ423-448 and S424A were ectopically expressed together with Myc-RAP74-CTD in HEK293T cells. After 48 hours, cells were lysed in hypotonic protein lysis buffer, containing 0.5 % NP-40, 10 mM Tris-HCl pH8, 60 mM KCl, 1 mM EDTA and complete protease inhibitors (Roche). DMSO or 1nM DHT (Sigma) were administered to the medium and the cells treated for 24h. Total cellular lysate was fractionated in mini-Protean TGX 4-20% acrylamide gel (Biorad) and blotted onto a nitrocellulose membrane (Amersham). Protein levels were assessed by means of the following antibodies: anti-β-actin-HRP, anti-Androgen Receptor (N-20), rabbit-anti-Flag, mouse-anti-Myc.

Proximity Ligation Assay (PLA)

HEK293T cells were grown on 12 mm-diameter coverslips (Thermo Scientific) in 6-well plates and transfected with 0.5 μg of each plasmid following a ratio of 1 μg DNA to 3 μl PEI for 48 hours. When mentioned, transfected cells were then incubated with 1 nM DHT for an additional 24 hours. Cells were fixed in PBS containing 4% Paraformaldehyde (EMS) for 10 minutes, subsequently washed in PBS and permeabilized with methanol for 5 minutes. Slides were blocked in PBS containing 0.1% Tween and 2% Bovine Serum Albumin (Sigma), and incubated with Flag and Myc-specific antibodies (Rabbit-anti-Flag and Mouse-anti-Myc). Cells were subsequently incubated with Duolink II PLA probes and stained according to manufacturer's protocol. Cells were analyzed with a 63× objective lens on a Leica SP5 or SPE confocal microscopes.

Localization Studies

HEK293T cells were grown on 12 mm-diameter coverslips and fixed in PBS containing 4% paraformaldehyde, and permeabilized in methanol. Cells were stained with a Flag-specific antibody (Rabbit-anti-Flag) in PBS containing 0.1% Tween, 2% BSA. Subsequently, cells were washed in PBS containing 0.1% Tween and incubated with goat anti-rabbit Alexa-Fluor 568 secondary antibody. After washing with PBS, cells were treated for 5 minutes with 5 mg/ml DAPI and mounted in Prolong Gold antifade (Thermo Fisher Scientific). Cells were analyzed with a 63× objective on a Leica SP5 or SPE confocal microscopes.

Transcriptional Activity Assay

To assess AR-mediated transcriptional activity on the Prostate Specific Antigen (PSA) promoter, HEK293T cells were co-transfected with pCMV5-Flag-AR WT or mutants, pTK-Renilla and PSA (6.1)-Luc plasmids, and 48 hours later were treated with 1 nM DHT for 24 hours. Samples were assayed for luciferase activity using the Dual-Luciferase Reporter Assay System according to manufacturer's instructions. pTK-Renilla was used for normalization of luciferase expression.

QUANTIFICATION AND STATISTICAL ANALYSIS

For the quantification of the PLA results, reported in Figure S3D, the spot count (foci) was used to assess differences between groups and treatments using a general linear model, including image batch of each experimental observation group as random effect.

For the reporter assay, reported in the Figure 3G, a general linear model was used to compare differences in log transformed PSA-Luc vs Renilla ratio between groups of interest using experiment batch, total cell count and replicate as covariates.